J Mater Sci (2011) 46:1424–1438
DOI 10.1007/s10853-010-4938-x

High thermal conductivity composites consisting of diamond filler with tungsten coating and copper (silver) matrix

Andrey M. Abyzov · Sergey V. Kidalov · Fedor M. Shakhov

Received: 22 March 2010 / Accepted: 18 September 2010 / Published online: 30 September 2010

Abstract Tungsten coatings with thickness of 5–500 nm are applied onto plane-faced synthetic diamonds with particle sizes of about 430 and 180 μm. The composition and structure of the coatings are investigated using scanning electron microscopy, X-ray spectral analysis, X-ray diffraction, and atomic force microscopy. The composition of the coatings varies within the range W–W_2C–WC. The average roughness, R_a, of the coatings' surfaces (20–100 nm) increases with the weight–average thickness of the coating. Composites with a thermal conductivity (TC) as high as 900 W m^{-1} K^{-1} are obtained by spontaneous infiltration, without the aid of pressure, using the coated diamond grains as a filler, and copper or silver as a binder. The optimal coating thickness for producing a composite with maximal TC is 100–250 nm. For this thickness the heat conductance of coatings as a filler/matrix interface is calculated as $G = (2–10) \times 10^7$ W m^{-2} K^{-1}. The effects of coating composition, thickness and roughness, as well as of impurities, on wettability during the metal impregnation process and on the TC of the composites are considered.

A. M. Abyzov (✉)
St. Petersburg State Institute of Technology,
Moskovskii pr. 26, Saint-Petersburg 190013, Russia
e-mail: andabyz@mail.ru

S. V. Kidalov · F. M. Shakhov
Ioffe Physical-Technical Institute of the Russian Academy of Sciences, 26 Polytekhnicheskaya st, Saint-Petersburg 194021, Russia
e-mail: kidalov@mail.ioffe.ru

Introduction

Certain forms of carbon have the greatest thermal conductivity (TC) among solid substances. At the same time, such carbon materials as pyrographite, carbon fibers, and nanotubes have a highly pronounced anisotropy of structure and, correspondingly, of TC. Thus, for graphite crystals at room temperature, the TC[1] reaches 1000–3000 W m^{-1} K^{-1} within the plane of the crystal layers, while perpendicular to the layers it is only 6 W m^{-1} K^{-1} [1–3]. Axial TC for carbon fibers made of pitch may reach 1200 W m^{-1} K^{-1}, and for chemical vapor deposited (CVD)-carbon fibers it may be as high as 2000 W m^{-1} K^{-1}, but their radial TC is much lower [2, 3]. Diamond in the form of pure defectless monocrystals has a TC of up to 2000–3000 W m^{-1} K^{-1}, while in practice the TC of diamond can be regarded as isotropic [1–3]. Measured along the axis, the TC of multi-walled carbon nanotubes is more than 3000 W m^{-1} K^{-1}, with a theoretical estimate of 6600 W m^{-1} K^{-1} for single-wall carbon nanotubes [1]. The materials currently used as heat sinks and thermal conductors in high-heat-flux systems are graphite, carbon fiber, and diamond; for the most part, nanotubes are still at the research stage. If TC anisotropy is not required, it is sensible to use diamond as a high heat conducting material. Powders and grains of natural diamond are not widely used as a technical raw material. Synthetic diamond is commercially available in the following basic forms:

– powders or grains, with particle or crystal size ranging from 5 nm to roughly 1 mm, which are produced at high pressures and temperatures under conditions of

[1] Here and below TC is considered at temperature about 300 K.

diamond thermodynamic stability and contain impurities of metals catalyzing graphite–diamond transition, generally Fe, Co, or Ni;
– polycrystalline compacts produced by sintering particles of diamond at high pressure;
– films, coatings, and layers produced by CVD under non-equilibrium conditions.

The polycrystalline compacts of diamond, obtained at pressures of more than 1 GPa and high temperatures, are limited as to their size and shape [4]. CVD-diamond is expensive and takes tens (hundreds) of hours to produce.

In most cases, materials with a high thermal conductivity are obtained in the form of composite materials, in which both the filler and the binder are substances with high TC. Composites with a filler of diamond particles may be made with a carbon, ceramic or metal binder (matrix). Diamond powders and grains of sufficiently high quality are available, owing to the large-scale production of such raw material for tooling and abrasive machining requirements.

The following relationships are universal for composites with diamond filler. The TC of the composite decreases if

– the volume fraction of the diamond filler diminishes, since the TC of the filler is higher than the TC of the matrix;
– the content of impurities (mainly nitrogen) in the diamond increases, as the TC of the filler decreases as a result;
– the diamond particle size reduces, since the filler/matrix interface, which has a finite thermal resistance, enlarges within the composite.

Cubic boron nitride, silicon carbide, and beryllium oxide have the highest TC among nonmetallic compound substances. The TC of BN_{cub}, SiC, and BeO monocrystals is 1300, 490, and 370 W m^{-1} K^{-1}, respectively [1]. The use of BeO is inexpedient due to its high toxicity. Producing boron nitride in its cubic form is as technically complex as diamond synthesis. Silicon carbide is used as a binder in composites with diamond filler. A widespread technique of composite production consists of the following stages: (1) the molding of a porous preform of the diamond powder (by pressing from slurry with or without an organic binder); (2) the heat treatment of this preform to form a semiproduct of diamond particles bonded with non-diamond carbon (CVD of pyrocarbon from hydrocarbons, carbonization of binder or partial diamond graphitization by heat treatment in a vacuum or with inert gas); (3) impregnation with the silicon melt to form silicon carbide by the reaction $C + Si \rightarrow SiC$.

For example, diamond–SiC–Si composites, with a residual silicon content ranging from 0.4 to 31%, were obtained from synthetic diamonds, with a dispersity varying from 3–5 μm to 50–63 μm, by siliconizing them in a vacuum at 1550 °C [5]. Using electron microscopy and electron diffraction it was found that there were many defects within a ~0.6 μm layer at the diamond/SiC interface, though the defect content of the diamond filler and the silicon carbide matrix in zones further from the interface was low [6]. The problem with producing composites with a nonmetallic binder is the complexity of ensuring a high TC in the binder, since the TC of ceramic materials declines sharply in the presence of impurities, defects, and any deviation from a monocrystalline structure. For example, while the TC of monocrystalline SiC is 300–490 W m^{-1} K^{-1}, for silicon carbide obtained by CVD it is 75–390 W m^{-1} K^{-1}; for reaction-sintered SiC it is 70–190 W m^{-1} K^{-1}; and for hot-pressed SiC it is 50–120 W m^{-1} K^{-1} [1]. If the TC of the binder is not sufficiently high, a composite with a high TC cannot be achieved, but it is very difficult to obtain a monocrystalline ceramic matrix.

Composites with a metal binder are obtained by the methods of infiltration of a melt or sintering. Silver and copper, which have the highest TC among metals (420 and 390 W m^{-1} K^{-1}, respectively) can be used as matrices for composites. Aluminum, which has a lower density and which is cheaper, but has the noticeably lower TC of 230 W m^{-1} K^{-1}, is also used. Aluminum is a carbide-forming element, though in the process of obtaining composites, when liquid aluminum is in contact with diamond, carbide forms only on the {100} faces of the diamond crystals [7]. Copper and silver are not carbide-forming metals, their melts do not wet the surface of carbon, and this is the main problem in obtaining diamond–Cu and diamond–Ag composites. For these reasons, and because diamond is a dielectric with a phonon mechanism of TC, whereas in metals heat is conducted by electrons, it is hard to achieve high adhesion and low thermal resistance at the filler/matrix interface. Thus, a number of reports are known, where the TC of obtained diamond–copper composites was about or even lower than the TC of the copper matrix [8, 9].

Diamond–copper composites can be obtained without the introduction of a third component by sintering or infiltration under high pressures >1 GPa. Thus, in [10] composites with a volume fraction of diamond of 50–80% and a TC of up to 740 W m^{-1} K^{-1} are obtained from powder mixtures of diamond, with particle size from 20–30 μm to 90–110 μm, and copper, by treatment at 4.5 GPa and 1150–1200 °C for a period of 15 min. Diamond–copper composites were sintered at 8 GPa pressure and 1600–1800 °C temperature [11]. With a diamond volume fraction of 90–95%, the TC of the composites increased from 240 to 900 W m^{-1} K^{-1} in line with the rise of diamond particle size from 7–10 μm to 425–600 μm.

Under milder sintering conditions, at 1–3 GPa, the diamond grains did not stay in the copper matrix, owing to bad adhesion. The authors of [11] proposed a structural model of the diamond grains within the composite material according to which the diamond consists of an internal core with an undistorted diamond structure and a TC of $\sim$1000 W m^{-1} K^{-1} and defective external shell, formed during sintering, with a thickness of $\sim$5 μm and a TC of $\sim$240 W m^{-1} K^{-1}.

Composites of diamond with a copper or silver matrix can be obtained without the application of high pressures >1 GPa, by making a thin transitional carbide layer at the diamond/metal interface. This can be achieved either by adding a small amount of a carbide-forming element into the metal of the binder or by the prior application of a coating of a carbide-forming metal onto the diamond surface.

Thus, the infiltration of a copper-based alloy with additions of chromium or boron was used by Weber and Tavangar [12]. As the concentration of the additions increased, the TC of the diamond–metal composite increased, peaking at a concentration of chromium in copper of 0.3 at.% and of boron in copper of 2.5 at.%, and then decreased. With a diamond volume fraction of 60%, and with a particle size of 200 μm, the TC of the diamond–Cr–Cu composite reached 600 W m^{-1} K^{-1}, while that of the diamond–B–Cu composite reached 700 W m^{-1} K^{-1} [12]. In [13], using a eutectic Ag–3 wt% Si alloy, composites with a TC of 775–860 W m^{-1} K^{-1} were obtained for monodisperse diamond fillers with a particle size of 350 and 450 μm, the volume fraction of diamond in the composite being 61–65%. A TC of 960–970 W m^{-1} K^{-1} was achieved for bidisperse fillers where the diamond particles were 450 and 52 μm or 350 and 52 μm in size and the volume fraction of diamond was 73–76%. Calculating the TC using the differential efficient medium (DEM) model showed that in the case of the monodisperse fillers, the theoretical TC limit of the composite had almost been reached [13].

In both cases [12, 13], infiltration of the melt into the dense diamond bed was assisted by gas pressure: heating and isothermal exposure were carried out in a vacuum at 10 Pa and an inert gas (Ar) was supplied at 0.5–5 MPa before cooling. In [14], a diamond–Cr–Cu composite was obtained and investigated. A mixture of 180–210 μm diamond grains and 0.8 wt% Cr–Cu alloy powder was sintered by pulse electric discharge to form a composite. The composite had a diamond volume fraction of $\sim$50% and a TC of 640 W m^{-1} K^{-1}. Using X-ray diffraction and electron microscopy it was determined that a layer of chromium carbide Cr_3C_2 with a thickness of 100 nm and a crystallite size of 20–40 nm had been formed at the filler/matrix interface, almost all the chromium from the alloy with copper having been changed into carbide. A diamond–Cu composite obtained with a binder of pure copper had a TC of only 200 W m^{-1} K^{-1}. In [15], diamond–copper composites were obtained by hot-pressing at 950 °C. Diamond, with a particle size of 100–125 μm, copper, and copper with the addition of 0.3–1.5 wt% of B, Cr, Al, Ti, or Zr was used. Additions of boron or chromium to the binder metal considerably increased the TC of the composite, aluminum slightly decreased the TC, and titanium and zirconium slightly increased it. Using a binder with a composition of Cu–0.8% Cr, the TC of a composite with the diamond volume fraction of 42% ranged from 490–515 to 590–640 W m^{-1} K^{-1}, depending on the heating technique used in sintering (indirect or direct). In comparison, the TC of a composite made with a pure copper binder was 215 W m^{-1} K^{-1}.

As can be seen from the references cited, the method of obtaining of diamond–copper and diamond–silver composites from alloys of copper or silver with a carbide-forming element is widely and successfully used. By contrast, there are a rather limited number of publications about the method, which uses a pre-coated diamond. For example, [15] describes the application of a molybdenum coating, with a thickness of 180 nm, to particles of silicon carbide measuring 30–70 μm to obtain SiC–Mo–Cu composites by hot-pressing with a binder of pure copper. The TC of the composite was 290 W m^{-1} K^{-1} as compared with 220 W m^{-1} K^{-1} for the SiC–Cu composite without a molybdenum coating. However, no data are available about similar experiments where coatings are applied onto diamond to obtain diamond–copper composites. The authors of [16, 17] applied a multilayer coating to diamond filler. Using physical vapor deposition, the diamond powder was coated first with a 10 nm-thick layer of a carbide-forming metal (W, Cr, Ti, Zr) and then with a layer of solder (Cu) 100 nm thick. Additionally, to improve the powder compactability, a copper layer was built up by "wet" electroless deposition to a thickness of several μm. A composite was then produced by the capillary infiltration of copper or a Cu–Ag alloy in a vacuum. A composite with a diamond particle size of 6–50 μm and a diamond volume fraction of 55%, with a first coating layer composed of W–26% Re, and a binder of Cu–80% Ag alloy had a TC of 420 W m^{-1} K^{-1} [16] (360 W m^{-1} K^{-1} according to the later report [17]). In [18], a chromium coating with a thickness of 1 μm was applied by vacuum deposition to diamond with a particle size of 100 μm. A composite was then produced on a copper binder using spark plasma sintering. With a filler volume fraction of 40–65%, the TC of the composite was less than 290 W m^{-1} K^{-1}. In [19], diamonds with particle sizes of about 40, 140, and 190 μm were coated by magnetron sputtering with a layer of a copper-based alloy with additions of a carbide-forming

element (Cu–0.5 wt% B, Cu–1 wt% Cr, Cu–3 wt% Si, Cu–4 wt% Ti), approximately 2 μm thick. Composites with a copper binder were also produced, using the spark plasma sintering method. With a filler volume fraction of 60–80%, the TC of the composite materials was not more than 300 W m^{-1} K^{-1}. Thus, these attempts [16–19] to obtain diamond–metal composites with a high TC by preliminary application of coatings to the diamond filler failed, since the materials obtained had a TC at the level or lower than that of the matrix metal.

The purpose of our work was to check experimentally the possibility of obtaining diamond–copper and diamond–silver composites with high TC exploiting the spontaneous infiltration (without the aid of pressure) by means of prior modification of the diamond fillers (applying a single layer of tungsten coating) as well as to investigate the structure and properties of the fillers and composites produced.

Experimental

High-quality synthetic diamonds, SDB 1085 35/45 (De Beers) and AS-160 200/160 (Intech Diamant),[2] with plane-faced cubic-octahedral monocrystalline particles, produced with an iron–nickel catalyst, were used. The nominal particle size was 350–500 μm for the SDB 1085 diamond and 160–200 μm for the AS-160 diamond. For synthetic plane-faced diamonds there is a known correlation between their habitus and color on the one hand, and their TC, within a range of 500–2000 W m^{-1} K^{-1}, on the other [20]. As per this correlation, the TC of the SDB 1085 and AS-160 diamonds used can be estimated as $\approx$1500 W m^{-1} K^{-1}. The estimation from Maxwell equation based on the experimental TC of the diamond–copper composite has shown that the intrinsic TC of the SDB 1085 35/45 diamond is not less than 1000 W m^{-1} K^{-1} [21]. Because of the presence of nitrogen impurity, the TC of commercial diamonds for powders intended for use as abrasives is less than 2000 W m^{-1} K^{-1} [13, 22].

Tungsten single-layer coatings were applied to diamond grains by the diffusion method [23, 24] at temperatures of 900–1100 °C. The thickness of the coatings ranged from 5 to 500 nm, depending on the treatment conditions. The quantity of the applied coating was measured gravimetrically by determining the increase in the diamond powder mass after applying the coating. Etching tests were also done by carrying out chemical removal of the coating in an alkaline solution of potassium ferricyanide (30.5 g $K_3Fe(CN)_6$ + 4.45 g NaOH + 100 mL H_2O, 15 mL of solution per 1 g of sample, 10 min with heating up to boiling). The results of determining the coating quantity by weight increment after deposition and by mass loss after etching coincided with an accuracy of 5%. Some of the coated diamonds were subjected to additional heat treatment (annealing) in a vacuum at 10 Pa, 1100 °C for 5 min.

Oxygen-free copper and silver were used as matrix metals. Metal purity was more than 99.9 wt%. Element analysis of the impurities in the metals was carried out by atomic-emission spectroscopy in inductively coupled plasma using a PS-1000 (Teledyne Leeman Labs); for sample preparation the metals were dissolved in nitric acid. The mass fraction of impurities in the copper was: B, Al, P, Co, Zn, Cd—less than 1 ppm; Si, S, Ti, Sn, Pb, As, Sb, Bi—less than 10 ppm; Cr—5 ppm, Mn—1 ppm, Fe—20 ppm, Ni—20 ppm, Ag—20 ppm. And in silver: Al, Co, Ni, Zn, Cd—less than 1 ppm; S, Sn, Pb, As, Sb, Bi—less than 10 ppm; Si—8 ppm, Fe—5 ppm, Cu—2 ppm.

Diamond–metal composites were obtained by top-infiltration of the metal melt into a dense bed of the pre-coated diamond particles. To produce the composites, 1 g of coated diamond was used; the ratio of the mass of the binder (metal) to the mass of filler (diamond with coating) C was maintained constant: $C = 1.50$ for the copper matrix and $C = 1.75$ for the silver one. These ratios ensure the highest possible volume fraction of diamond in the composite ($\approx$0.63 for a monodisperse filler in the case of zero porosity). Infiltration was carried out in a vacuum at a pressure of about 10 Pa, in graphite molds, and in a chamber made of chrome–nickel steel with induction-heated walls. The mold containing the filler-and-metal preform was heated from room temperature to the maximal temperature within 6 min. The impregnation temperature for copper was 1130 °C with a holding time of 5 min; for silver the temperature was 1000 °C and the holding time 10 min. Composite samples were obtained in the form of cylinders with a diameter of 5 mm and a height of 23–24 mm.

The diamond grains, with and without applied coatings, were investigated using scanning electron microscopy (SEM) with X-ray spectral microanalysis, X-ray diffraction, and atomic force microscopy (AFM). Images with a magnification of ×60… ×6000 were obtained using an electron microscope JSM-35CF (Jeol) with a Link 860 energy-dispersive attachment (Link) for element microanalysis. The coating thickness on individual facets was determined using the ratio of the tungsten line intensity of the coating to the tungsten line intensity of a volume standard (Yakowitz–Newbury method). To do this, electron probe X-ray spectral microanalysis of the coatings was carried out on $\approx$30 × 30 μm areas of various grains, taking 10 replicate measurements. The phase composition of the coatings was determined with X-ray diffraction. Diffractograms were

[2] Numbers written with a slash designate the granulometric composition of the powders; in the first case, in meshes, in the second, in micrometers.

taken using a Difray (Scientific Instruments) with a position-sensitive detector on Cu K_α radiation, with an incidence angle of the X-ray beam relative to the sample surface of 15° and an irradiated area of about 20 mm^2. The surface roughness was measured by scanning 30 × 30 μm areas on the facets of the diamond grains, using a Solver P-47 Pro atomic force microscope (NT-MDT).

Density, TC, and coefficient of linear thermal expansion (CTE) were determined for the composite samples produced. Density was measured using a pycnometer with an accuracy of 1% and with water as the operating fluid. The absence of open porosity was confirmed visually using an optical microscope. TC was measured using the steady-state axial heat flux technique [21], taking 5–7 independent measurements at 60–70 °C. Namely, the TC was measured by an absolute method in a vacuum (pressure 3 Pa). The sample-rod was clamped vertically between two copper cylinders. The vertical heat flow through the cylinder-sample-cylinder was determined by means of thermocouples assembled in the copper cylinders. The vertical gradient of temperature for the sample was measured by two another thermocouples, which were mounted on the external surface of the samples without drilling holes. The results of measurements of the TC of a copper standard, of 99.9 wt% purity and of the same size as the composite samples (∅5 × 25 mm), are shown in Fig. 7. The TC value measured for the copper standard, (383 ± 18) W m^{-1} K^{-1}, coincides with the reference data [25]. The average CTE, within a temperature range from 20 to 300 °C, was measured in a dilatometer with an accuracy of 5%.

Results

The diamond particles kept their initial shape after applying the coating. Particles of SDB 1085 diamond are mostly regular polyhedrons, whereas for AS-160 diamond, the number of particles with defects (chips, large growth steps, etc.) was greater (Fig. 1). According to SEM and X-ray spectral microanalysis, all the coatings produced are continuous, and the heterogeneity of the coatings is apparent, starting from a scale of the order of 10 μm (Fig. 2). Additional heat treatment in a vacuum at 1100 °C has an insignificant effect on the coating morphology.

According to AFM, the initial SDB 1085 and AS-160 diamonds have pores similar to etching pits with diameters ranging from fractions of μm to several μm, extending from the surface into the interior of the particles. After coating deposition, clearly defined pores were not observed.

Images of the surface of SDB 1085 diamond, in its initial state and with a 110 nm coating, obtained by AFM, are shown in Fig. 3. In Fig. 3a, one can see a growth step and pores on the smooth facet of initial diamond. With a coating thickness in the range of 50–500 nm, the coating surface texture on the SDB 1085 diamond is similar to that depicted in Fig. 3b and has a continuously lumpy character. At the same time, the mean roughness, R_a, of the coating surface increases linearly with the weight–average thickness of the coating (Fig. 4), reaching about 100 nm at a coating thickness of 500 nm. The mean (arithmetic average) roughness, R_a, characterizes the surface texture, being the extent of deviation from an ideally smooth surface, is measured as the mean value of absolute deviations of the profile from the baseline. The R_a/h ratio is an additional characteristic of texture. For a substrate with zero roughness, $R_a/h < 1$ may be taken as the condition of continuous coating. As can be seen from Fig. 4, the R_a/h ratio for the coatings obtained is between 0.1 and 0.3 for coatings with a thickness of at least 100 nm. For SDB 1085 diamond, the coating roughness increases appreciably with coating

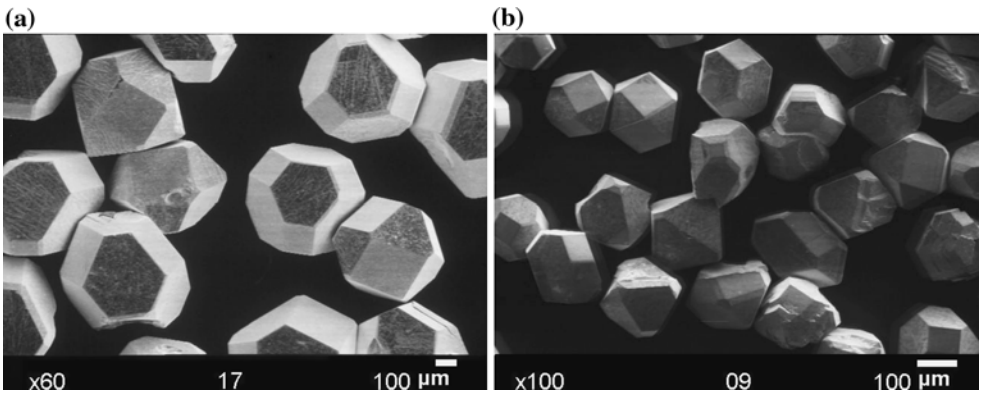

Fig. 1 Particles of SDB 1085 35/45 diamond with a coating of 150 nm thickness (**a**) and AS-160 200/160 diamond with a coating of 130 nm thickness (**b**). SEM in secondary electrons

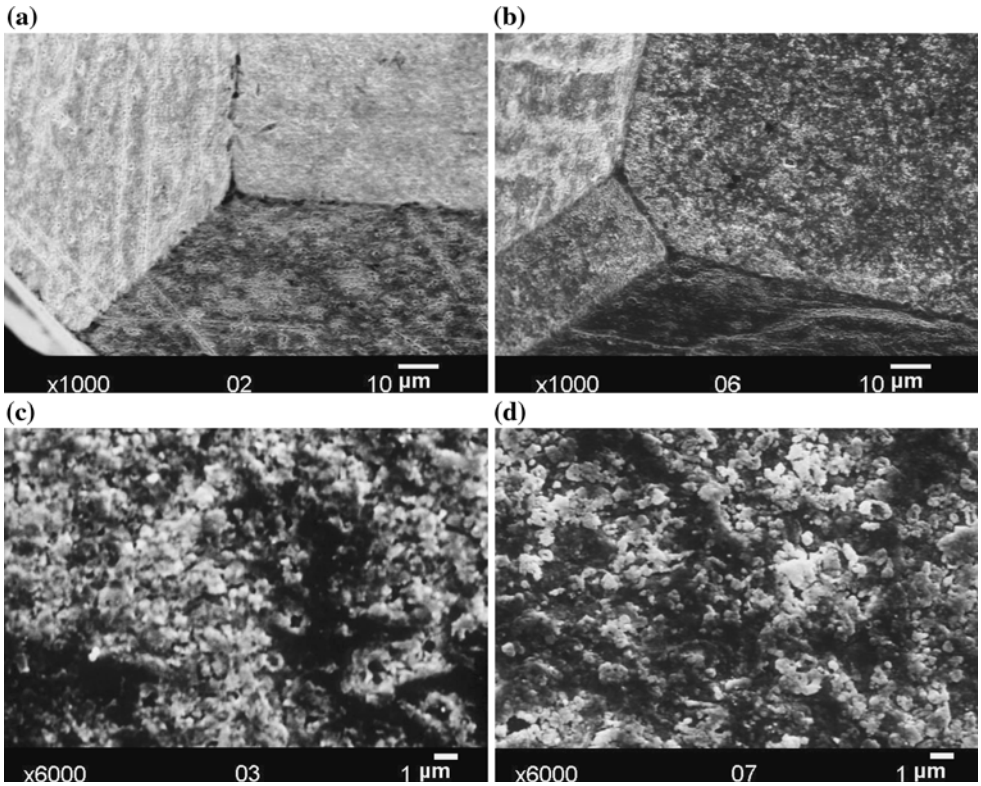

Fig. 2 Surface of SDB 1085 35/45 diamond with coating of 150 nm thickness: **a** and **c** after applying coating; **b** and **d** after additional heat treatment at 1100 °C for 5 min in a vacuum. SEM in secondary electrons

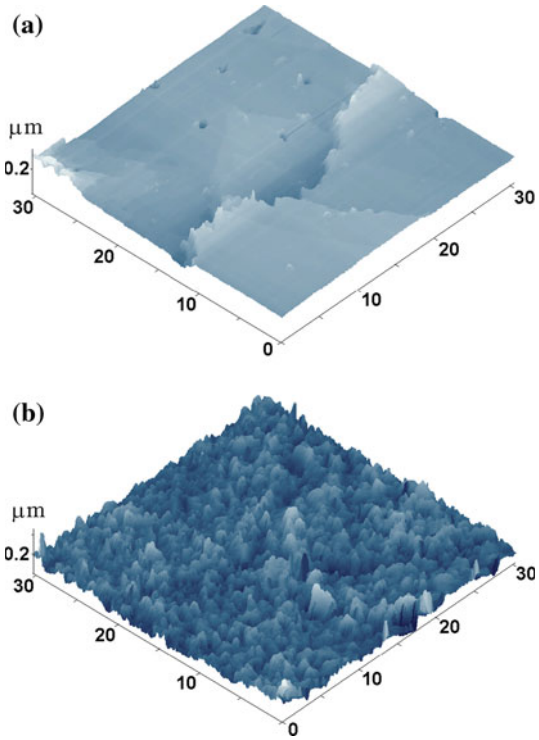

Fig. 3 AFM images of the surface of SDB 1085 35/45 diamond **a** in its initial state and **b** with a coating of 110 nm thickness

thickness, while for AS-160 diamond R_a rises slightly with h, and absolute values of roughness for the AS-160 are lower than for the SDB 1085.

Examples of diffractograms of the initial diamonds, diamonds with a coating, and diamonds with a coating after heat treatment are presented in Figs. 5 and 6.[3] For SDB 1085 diamond with coating thickness of 50 nm and above, metal tungsten (W) is the dominating phase of the coating, and the content of carbides (W_2C, WC) in the coating is insignificant. The annealing of diamond with a tungsten coating results in the carbidization of the coating; the diamond carbon of the substrate grains interacts with the tungsten of the coating to form tungsten semicarbide and monocarbide:

$$2W + C_{diamond} = W_2C \quad (1)$$

$$W + C_{diamond} = WC \quad (2)$$

$$W_2C + C_{diamond} = 2WC \quad (3)$$

In the case of SDB 1085 diamond with a coating thickness of at least 50 nm, after heat treatment (1100 °C, 5 min) all three phases, WC, W_2C, and W, are present in the coatings, and the thicker the coating, the higher the content of metal tungsten and the lower the content of monocarbide WC. For AS-160 diamond, in comparison with SDB 1085 diamond the applied coatings contain more tungsten semicarbide, so that at a thickness of 100–200 nm they consist of W and W_2C in comparable quantities. As a result of heat treatment, coatings on the AS-160 become carbidized to a

[3] Identification by PDF database: 6-675* diamond, cub. lattice; 4-806* W cub.; 35-776* W_2C hex.; 25-1047* WC hex.

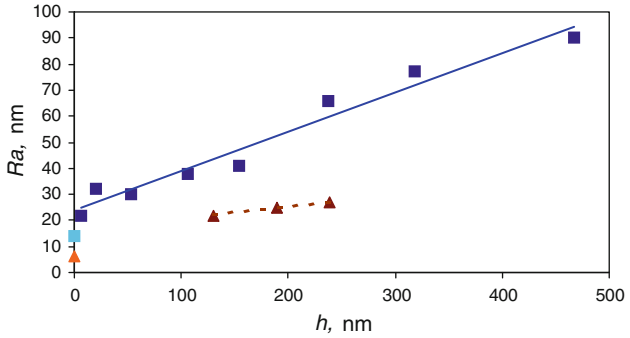

Fig. 4 The average roughness of the surface of coatings on SDB 1085 35/45 diamond without annealing (*squares*) and on AS-160 200/160 diamond after annealing (*triangles*) versus the weight–average thickness of the coating. Two points at $h = 0$ correspond to the initial diamonds without coatings

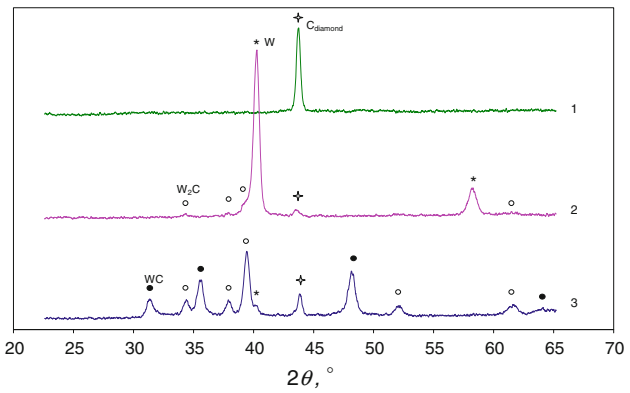

Fig. 5 X-ray diffractogram of SDB 1085 35/45 diamond: *1* initial, *2* with a tungsten coating of 150 nm thickness, *3* with a coating after heat treatment in a vacuum (1100 °C, 10 Pa, 5 min)

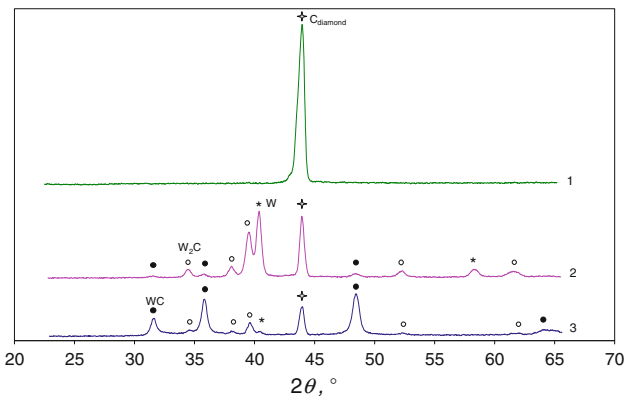

Fig. 6 X-ray diffractogram of AS-160 200/160 diamond: *1* initial, *2* with a tungsten coating of 130 nm thickness, *3* with the coating after heat treatment in a vacuum (1100 °C, 10 Pa, 5 min)

greater extent (i.e. contain more WC) than coatings on the SDB 1085. Graphite-like carbon was not detected anywhere either before or after heat treatment of the coating.

For AS-160 and especially SDB 1085 samples the diffraction peak C{111} near 44° was registered with poor reproducibility due to the large size of the diamond particles[4] and the regular plane-faced shape of these particles. It is connected with the fact that an insufficiently large number of crystals meet the X-ray beam, and grains in the cuvette may lie not in a random manner. Yet, the diffractograms of the coatings are registered reliably. The mass absorption coefficients of Cu K_α radiation for carbon and tungsten are $\mu^*_C = 4.51$ cm^2/g and $\mu^*_W = 168$ cm^2/g [26]. The linear absorption coefficients $\mu = \rho\mu^*$ are $\mu_C = 15.8$ cm^{-1} and $\mu_W = 3240$ cm^{-1}, respectively. The penetration depth of X-radiation $1/\mu$ is 630 μm (diamond substrate) and 3.1 μm (tungsten coating). The coating is therefore analyzed through its whole depth ($1/\mu_W \gg h$, where h is the coating thickness), and the recording is carried out from the powder bed with the thickness of one or several diamond particles ($1/\mu_C \geq D$, where D is particle diameter). With a coverage area of $\sim$20 mm^2, the diffractogram is registered from more than 10^2 particles in the case of the more coarsely dispersed diamond, SDB 1085 35/45. The problem of the heterogeneity of the phase composition of the coating, i.e. how phases W, W_2C, WC are distributed over various diamond particles, over the various facets of individual particles, over an area and throughout the depth of the coating layer on the individual facets, needs further investigation.

As a measure of the quantity of coating applied to particles in the course of the present research we use the value of the equivalent weight–average thickness of an ideal smooth homogeneous film of metal tungsten h, nm

$$h = \frac{m_W}{\rho_W m s} 10^3 \quad (4)$$

where m_W (g) is the tungsten mass in the coating, $\rho_W = 19.3$ g/cm^3 is the tungsten density, m (g) is the diamond mass, s (m^2/g) is the specific geometric surface of diamond particles. The value h is convenient for comparing a number of coatings with differing roughness and phase composition. The real thickness of the coating varies, changing from one point to another due to heterogeneity and roughness. For carbide coatings, the weight–average thickness of tungsten can be recalculated into the weight–average thickness of corresponding carbide. For example, in the limit of the tungsten monocarbide coating $h_{WC} = (M_{WC}/M_W)(\rho_W/\rho_{WC})h = 1.32\,h$, where $M_{WC} = 195.85$ g/mol and $M_W = 183.84$ g/mol are the molar masses of WC and W, $\rho_{WC} = 15.6$ g/cm^3 is the density of WC. Since coatings can be multiphase (W–W_2C–WC) and have a less than monocrystalline density, due to the presence of defects, then a detailing of thickness determination seems to be unreasonable in the aspect of general characteristic of the coating quantity which is of interest to us here. The specific

[4] Optimal for powder diffractography particle size is several μm.

geometric surface area of diamond particles was calculated by the ratio

$$s = \frac{6}{\rho_d D \psi} \quad (5)$$

where $\rho_d = 3.52$ g/cm^3 is the diamond density, $D = (D_{min} + D_{max})/2$ (μm) is the median-average size of the diamond particles, $\psi = 0.7$ is the form-factor (ratio of the surface area of a sphere of equal volume to the particle surface area). The value of $\psi = 0.7$ is a mean for the various powders used in practice, whose particle geometry is not anisotropic [27]. For the morphological series of regular polyhedrons of synthetic diamond crystals cube–cuboctahedron–octahedron–rhombododecahedron [28], a calculation of the form-factor ψ gives the following values: 0.806–0.905–0.846–0.905. Deviations from the ideal geometric shape and defects (chips, growth steps, etc.) decrease the value of ψ. The calculated value of s is equal to 0.0057 m^2/g for SDB 1085 35/45 diamond and 0.014 m^2/g for AS-160 200/160 diamond.

The weight–average thickness of the coatings determined by gravimetric data and characterizing a powder sample as a whole (1–10 g), coincided with the local weight–average thickness of coatings on facets of individual particles found by X-ray spectral microanalysis, with deviations within ±20%.

Data on the properties of the diamond–metal composites obtained are listed in Table 1. The density of the ideal nonporous composite is calculated by the ratio

$$\rho* = \frac{1 + C}{\frac{(1-x)}{\rho_d} + \frac{x}{\rho_c} + \frac{C}{\rho_m}} \quad (6)$$

where C is the mass ratio of the metal to the coated diamond, x is the mass fraction of the coating on the diamond, $\rho_d = 3.52$ g/cm^3 is the diamond density, $\rho_c = 19.3$ g/cm^3 is the coating density (W), ρ_m is the matrix metal density (8.92 g/cm^3 for copper and 10.49 g/cm^3 for silver). In the absence of a coating ($x = 0$), $\rho* = 5.53$ g/cm^3 for the copper matrix and $\rho* = 6.10$ g/cm^3 for the silver matrix; taking the coating into account ($x \leq 5\%$ for fillers used) somewhat increases $\rho*$. According to the observations made with the optical microscope, there was no open porosity in the composite samples. The closed porosity of the composite ε is calculated by the equation

$$\varepsilon = 1 - \frac{\rho}{\rho*} \quad (7)$$

where ρ is the pycnometric density of the sample. The volume fraction of diamond v_d in the composite is

$$v_d = \frac{1 - x}{1 + C} \cdot \frac{\rho}{\rho_d} \quad (8)$$

Figure 7 illustrates the dependence of composite TC on the thickness of the coating applied to the diamond filler.

One group of the composite samples on a copper matrix is obtained from diamond filler with a directly applied tungsten coating; another group is obtained from filler with a coating, which has undergone additional heat treatment.

Table 1 The properties of metal matrix composites on the basis of a diamond with a tungsten coating and the conditions for producing them

Matrix	Diamond	Coating thickness h (nm)	Heat treatment[a]	Composite				
				Pycnometric density ρ (g/cm^3)	Closed porosity ε (%)	Diamond volume fraction v_d	TC[b] λ (W m^{-1} K^{-1})	CTE α (ppm/K)
Cu	SDB 1085	110	–	5.54	0.4	0.63	907 ± 11	6.9
		130		5.46	2.0	0.62	830 ± 16	
		150		5.42	2.8	0.61	741 ± 73	
		170		5.50	1.5	0.62	731 ± 21	
		240		5.54	1.2	0.62	597 ± 31	
		320		5.51	2.2	0.62	579 ± 42	8.3
		470		5.59	1.6	0.62	476 ± 22	
		50	+	5.21	6.1	0.59	723 ± 36	
		150		5.51	1.2	0.62	648 ± 59	
	AS-160	130	+	5.50	2.3	0.62	679 ± 9	7.6
		190		5.47	3.5	0.61	700 ± 14	
		240		5.48	4.0	0.61	767 ± 8	
Ag	SDB 1085	110	–	5.52	10.1	0.57	847 ± 58	
		240		5.99	3.1	0.61	834 ± 44	8.6
	AS-160	130	–	5.80	6.6	0.59	646 ± 60	9.7

[a] Diamond after coating deposition was annealed in a vacuum (1100 °C, 10 Pa, 5 min)

[b] Confidence limits with the confidence level of 0.05 are indicated

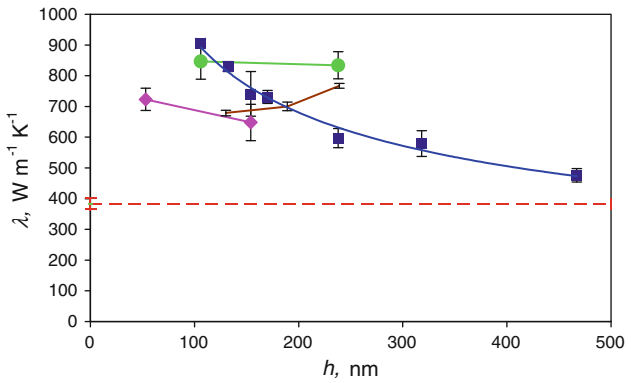

Fig. 7 The TC of diamond–metal composites versus the weight–average thickness of the tungsten coating on the diamond: SDB 1085—Cu (*squares*), SDB 1085 with annealed coating—Cu (*rhombs*), SDB 1085—Ag (*circles*), AS-160 with annealed coating—Cu (only *error bars*) (Table 1). *Dash line* is the TC of a copper etalon

The temperature of this heat treatment (1100 °C) was close to the temperature of the copper infiltration (1130 °C), and so in the case of the fillers which had undergone prior heat treatment, the structure and phase composition of the coatings have been stabilized and should not noticeably change during the process of infiltration. But when fillers which have not been annealed are used, the carbidization of the tungsten coating on the diamond should run during the process of heating performed to produce the composite. Probably, in the latter case the degree of carbidization of the tungsten coatings, being a part of the formed composite is roughly the same as after the heat treatment in a vacuum. Heat treatment had little effect on the coating surface roughness. So, for SDB 1085 diamond with a coating of 150 nm thickness, R_a was 41 nm without annealing and 36 nm after annealing; for AS-160 diamond with a coating of 240 nm thickness, R_a was 28 nm without annealing and 27 nm after annealing.

The composites obtained have low residual porosity and a roughly the same diamond volume fraction of 0.60 ± 0.03. For the composite obtained from SDB 1085 diamond with a copper matrix, the dependence of the TC on the thickness of the tungsten coating was investigated extensively. If the thickness of the coating was too small, we failed to obtain a composite, or the composite produced was of bad quality. Thus, with tungsten coatings of $h = 6$ nm, a copper infiltration into a bed of coated SDB 1085 diamond did not run, while for $h = 20$ nm the composite had cavities and some grains broke down out of the sample. Such behavior was observed with non-heat-treated coatings up to a thickness of 100 nm for SDB 1085 diamond. We succeeded in obtaining a robust composite, if SDB 1085 diamond with a coating as thin as 50 nm was additionally annealed. But additional heat treatment of coated SDB 1085 diamond reduced the TC of the composite. For SDB 1085 diamond with a 150 nm coating without annealing, the TC of the composite reached 740 W m^{-1} K^{-1}, while in the case of additional heat treatment the TC fell to 650 W m^{-1} K^{-1} (Table 1).

Discussion

Let us consider the data obtained as they pertain to the way the process of infiltration is carried out and the TC of the composites produced.

Wettability is a necessary condition of melt spreading (pressureless infiltration in the case of particle bed impregnation):

$$0 \leq \theta < 90^\circ \tag{9}$$

where θ is the contact angle of a liquid on a solid surface. Diamond is not wetted by the melts of metals belonging to the IB Group of Periodic Table. Values of wetting angles are represented in Table 2. As can be seen from the table, wetting angles are less on diamond facets {111} and increase with surface roughness.

Thus, if infiltration is carried out using metal melts which do not wet diamond and do not contain carbide-forming additives; it is necessary to modify the diamond surface by applying a coating, which ensures wettability.

As a general rule, the following factors influence the wettability by a metal melt of a coating applied to a non-metal (diamond):

- phase composition (metal or carbide) and possible heterogeneity of the chemical composition of the coating;
- coating thickness, if it is less than hundred(s) of nm;
- coating roughness;
- the presence of impurities in the coating and melt (especially on their surfaces).

The same factors determine the TC of the composites obtained.

Coating composition

The wetting angle of copper on bulk metal tungsten in a high vacuum (pressure 3×10^{-3} Pa) is 39° at 1150 °C,

Table 2 Contact angle of copper at 1100 °C and silver at 1000 °C on carbon materials in a vacuum at 10^{-3} Pa [29]

Substrate	Roughness (nm)	θ (°)	
		Cu	Ag
Diamond {111}	10	138	134
	50	158	146
Diamond {100}	10	147	142
Graphite MPG-6	–	143	127

29° at 1250 °C, and 0° at 1350 °C [30]. The decrease in the wetting angle with increasing temperature is explained by the desorption of surface oxides from tungsten, which oxides worsen the wetting.

The wetting angle of copper on tungsten carbide is small and lower than on most other carbides (Table 3). The wetting angle of copper on molybdenum carbide Mo_2C at 1130 °C is 40° [31].

Our experiments are carried out at a pressure of about 10 Pa, when oxygen content in the gas phase is higher, and so one can expect a certain increase in the value of the wetting angle in comparison with a high vacuum. In a high vacuum at relatively low temperature (1150 °C) the wetting angle on tungsten carbide WC (17°, see Table 3) is lower than that on metal tungsten (39° [30]). However, composite production at a temperature of 1130 °C showed that additional heat treatment of the coated diamond, which was accompanied by coating carbidization, did not result in an improvement in wetting.

The TC of metal tungsten is 174 W m^{-1} K^{-1}, and so tungsten follows aluminum (230 W m^{-1} K^{-1}) in the scale of metal TC. Molybdenum has a TC close to that of tungsten. In a sequence of other transitional elements of IV–VI Groups from chromium to titanium, TC decreases from approximately 100 to approximately 20 W m^{-1} K^{-1} (Table 4).

The TC of tungsten carbides is higher than that of other metal-like (non-covalent) carbides (Table 5).

The wide range of TC values of tungsten monocarbide given by various sources is probably due to differences in the structure of the samples investigated: TC increases as the structure of the material approaches a monocrystalline state. It is evident that for tungsten the highest TC value of the monocarbide, WC, is fairly close to the TC of the metal. (For some other elements — Zr, Hf, Ti, V — the TC of their carbides is also on a level with the TC of the corresponding metals).

In our case, for heat-treated SDB 1085 diamond with a 150 nm coating, the TC of the composite was somewhat lower than without such heat treatment (Table 1), i.e. increasing the degree of carbidization of the coating resulted in a decrease in TC.

It is also possible to conclude that tungsten is preferable among carbide-forming elements to use as a coating on the diamond filler for copper matrix infiltration, as tungsten ensures better wettability and higher TC. On the one hand, tungsten forms carbide, which is wetted better than the carbides of other transitional elements. On the other hand, tungsten's carbidization rate is lower than that of other metals (Ti, Zr, Nb, Cr, Mo, and others), due to a lower coefficient of carbon diffusion in tungsten [31]. In the case of a copper matrix, the process of infiltration required heating to a temperature higher than the melting point of Cu (1084 °C) for a period of several minutes. Partial or complete carbidization of the thin metal film applied to the diamond is unavoidable under these conditions.

Tungsten (as well as molybdenum) and copper (or silver) are practically mutually insoluble and do not form chemical compounds. During the infiltration of the matrix metal, therefore, the tungsten coating on the diamond is not washed out by the melt, elements, which could decrease the TC of the matrix, do not diffuse from the coating into the matrix, and a distinct coating/matrix interface is formed. The solubility of tungsten in copper at 1300 °C is 0.1 ppm (at.) [35]. The solubility of carbon in copper at 1150 °C is 26 ppm (at.) [36] and obviously does not influence the production of the composite or its properties [37].

Taking the above into consideration, of all the elements from which coatings can be formed on diamond, only tungsten, and probably molybdenum, can be expected to ensure the possibility of obtaining high TC composites with a copper or silver matrix by spontaneous infiltration (without the aid of pressure).

Coating thickness

It is well known that two specific factors influence the properties of thin films: (1) their continuous or discontinuous structure; (2) size effects, i.e. the influence of the film's thickness, h, and the size of the grains, L, of which it consists, on its physical properties (including conductivity).

Table 3 Contact angle of copper on bulk carbides in a vacuum at 1×10^{-3} Pa at 1150 °C [32]

Carbide	WC	VC	Cr_3C_2	NbC	TiC	ZrC	HfC
θ (°)	17	45	50	58	113	128	134

Table 4 Thermal conductivity of carbide-forming metals [33]

Metal	W	Mo	Cr	Ta	Nb	V	Zr	Hf	Ti
λ (W m^{-1} K^{-1})	174	138	94	58	54	31	23	23	22

Table 5 Thermal conductivity of carbides of metals [31, 33, 34]

Carbide	WC	W_2C	MoC	Mo_2C	VC	HfC	TaC	ZrC	TiC	Cr_3C_2	NbC
λ (W m^{-1} K^{-1})	29–121	29–36	24	7–32	25	22	22	21	17–21	13–19	14

Both h and L growth leads to an increase in TC, because the scattering of heat carriers on the surfaces of the film and grains reduces. Meanwhile, the upper boundary for the characteristic sizes of L and h, at which these effects are observed, is not limited to 100 nm, the standard cut-off value for allocation of nanostructures [38], and may be 1 μm and more (especially with phonon TC) [39, 40].

No loss of continuity was observed down to a minimum thickness of $h = 6$ nm for the coatings we obtained, but size effects should appear more or less. The mean free path, l, at a temperature of 300 K is about 100 nm for phonons in monocrystalline diamond [41] and 42 nm for electrons in copper [40]; the value of l for bulk tungsten or tungsten carbide is of the same order. Thus, the mean free path of heat carriers in the filler (diamond), in the coating on the filler/matrix interface, and in the matrix is comparable with the thickness h of the coating (Table 1) and with the size of the grains of which the coating is composed.

From our experimental data for SDB 1085 diamond and a copper binder, it follows that, as the coating thickness decreases down to values less than 50 nm, the coated diamond ceases to be wetted by the copper, i.e. the wetting angle increases up to the value of $\theta > 90°$.

This qualitative result can be compared with measurements of the wetting angle of metal melts on thin metal films applied onto oxide and carbon substrates [29, 42, 43]. Molybdenum films with a thickness of 5–300 nm were deposited by vacuum evaporation on quartz SiO_2, sapphire Al_2O_3, and graphite. The effect of film thickness, h, on the wetting angle of copper or copper saturated with molybdenum was measured at 1150 °C in a high vacuum (10^{-3} Pa). The critical film thickness, below which a decrease of h resulted in the wetting angle, θ, beginning to increase sharply, i.e. a worsening of the wettability, was $\approx$20 nm for the graphite substrate and $\approx$40 nm for the oxide substrates. The observed dependence $\theta(h)$ was explained by a loss of continuity with the decrease in film thickness (a transition to a discontinuous film structure), as well as by the accompanying changes in film roughness.

The contact angle of Cu–Ni–Mn melt on carbon substrates (graphite and diamond) coated with a molybdenum film up to 250 nm thick was measured at 1050 °C in a vacuum at 7×10^{-3} Pa. The critical film thickness, below which the wetting angle sharply increased, was about 50 nm, with the wetting angle depending slightly on the substrate material (the difference in the value of θ for diamond and graphite was not more than 10°). Naidich and others [29, 43] also carried out direct capillary infiltration of Cu–Ni–Mn alloy into a particle bed of ASK 160/125 synthetic diamond with a molybdenum coating applied by the diffusion method at 950 °C. Infiltration is reported with a coating thickness of not less than 70 nm, stable impregnation taking place where $h \geq 150$ nm. It should be noted that in our case the threshold thickness of tungsten coating on SDB 1085 35/45 diamond for ensuring pressureless infiltration was lower than these h values.

As regards TC, the decrease in the TC of the composite with the increase of coating thickness appears quite usual, since the TC of applied tungsten coatings, whether metal or carbide, ($\leq$170 W m^{-1} K^{-1}), is lower than that of the diamond filler ($\sim$1500 W m^{-1} K^{-1}) and of the matrix (390 W m^{-1} K^{-1} for Cu and 420 W m^{-1} K^{-1} for Ag). For bulk materials (thick films), the thermal resistance[5] of the layer R is proportional to its thickness: $R = h/\lambda_s$, where λ_s is the TC of the layer. Accordingly, the increase in the thickness of a tungsten coating, which attributed to a "thick" film, should lead to a decrease in the TC of the composite. This behavior is observed for a composite consisting of SDB 1085 diamond and a copper matrix (see Fig. 7). Thus, the TC falls to 480 W m^{-1} K^{-1} when $h = 470$ nm, i.e. with a coating thickness of about 500 nm, the TC of the composite is reduced to the TC of the matrix.

By contrast, for a composite from AS-160 diamond, which has been annealed after coating deposition, the dependence of TC on coating thickness h is reversed: the TC rises with h throughout the investigated range of 130–240 nm. For a composite of SDB 1085 with a silver matrix, samples with coating thickness of 110 and 240 nm have the same TC within a measurement error ($\sim$840 W m^{-1} K^{-1}, Fig. 7). Obviously the unexpected increase or constancy observed in TC with the increase in h is connected with size effect, namely the dependence of the TC of a coating on the size of its grains and its thickness. In this case the TC of the coating seems to increase with h so quickly that the thermal resistance of the coating does not increase, or even decreases, as a result.

Coating roughness

It is difficult to predict the influence of coating roughness on their wettability by melts. The known Wenzel–Deryagin equation states:

$$\cos(\theta) = r \cos(\theta_0) \tag{10}$$

where θ_0 and θ are the contact angles of a liquid on smooth and rough surfaces and r is the roughness coefficient equal to the ratio of the actual surface area to its projection. According to (10), roughness improves wetting ($\theta < \theta_0$) at $\theta_0 < 90°$ and worsens ($\theta > \theta_0$) at $\theta_0 > 90°$. However, as experimental investigations show, Eq. 10 is not always fulfilled [29]. It is correct to apply the Wenzel–Deryagin

[5] Thermal resistance is determined as ratio $\Delta T/q$, where ΔT (K) is temperature fall, q (W/m^2) is heat flow. Inverse to thermal resistance value $G = 1/R$ is called heat conductance and is measured in W m^{-2} K^{-1}.

equation if the drop size is 2–3 orders of magnitude greater than the scale of surface heterogeneity [44]. The evaluation shows that in our case this requirement is fulfilled. For example, for infiltration into a bed of particles with a size of ~100 μm and surface roughness of ~100 nm, we have a ratio R_a:d ≈0.1 μm:10 μm ≈10^{-2}. Here d is the characteristic measurement of the space between the particles in the bed (the equivalent diameter of the narrowest channels for the flow of liquid), having the order of 1/10 of the particle diameter D. According to experimental data [45], the surface roughness of metal tungsten does not influence the angle of wetting by copper in regions of both nonwettability ($\theta > 90°$) and wettability ($\theta < 90°$).

The TC of the composite depends on the thermal resistance of the diamond/coating and coating/matrix interfaces. The roughness of these interfaces decreases its effective (related to the area of smooth surface along the perimeter of particles) thermal resistance due to an increase of medium contact area. As follows from Fig. 4, for SDB 1085 diamond, the roughness of the coating/matrix interface increases considerably with the growth of coating thickness, which can partially compensate the increase in thermal resistance of the coating itself.

Impurities, diffusion

Any impurity decreases the TC of the diamond filler and the matrix metal.

Elements are ranged according to the decrease of the influence of the atomic percentage of impurity on the electro- and thermal conductivity of copper, as follows [25]: Ti, Fe, S, P, Co, As, Sb, O, … Oxygen is the most universal and mobile pollutant. For the content in copper of up to ~0.05 wt% O, oxygen has a weak influence on the TC of the copper (the TC decreases by a value of up to ~5 W m^{-1} K^{-1}). Oxygen is poorly soluble in solid copper, but liquid copper dissolves oxygen and at 1065 °C eutectic Cu–Cu_2O (mass fraction of 3.9% Cu_2O or 0.44% O) forms. The melting temperature for cupric oxide (CuO) is 1122 °C, while for cuprous oxide (Cu_2O) it is 1225 °C [36]. Oxygen in copper with the content of 0.025 wt% O or in the form of surface oxide on tungsten significantly worsens tungsten wetting by copper [45]. Silver in its solid state hardly dissolves oxygen at all, but in its liquid state, on the contrary, silver dissolves oxygen well. Tungsten forms with oxygen a number of oxides with composition from WO_2 to WO_3 [46].

In order to prevent the negative effect of oxygen we used oxygen-free copper, the process of infiltration was carried out in a vacuum; applied tungsten coatings were controlled by X-ray diffraction to ensure tungsten oxides were not present. The purity of the copper and silver used was 99.9%, with the content of individual impurity elements up to 20 ppm (wt.), which meets the requirements for obtaining composites with a high TC.

In contrast to the matrix metal and the metal–carbide coating, contamination of the diamond filler with impurities in the process of coating deposition and melt infiltration is not a danger. When a coating is deposited or heat treated, carbide formation takes place, owing to the diffusion of carbon atoms into the coating (W, W_2C), but the reverse diffusion of tungsten atoms into diamond is practically non-existent. In principle, the process of diffusion deposition of coatings is accompanied by the appearance of vacancies, micropores or dislocations in the sub-surface diamond layer [29]. However, for the coatings we obtained, with thickness of up to 100–250 nm, the influence of diffusion loosening of the diamond on the TC of the material is probably insignificant.

The TC of diamond crystals is mainly determined by the content of nitrogen impurity in them, and so if the atomic fraction of nitrogen increases from ~10 to ~300 ppm, the TC of synthetic diamonds decreases from 2000 to 500 W m^{-1} K^{-1} [20]. The effect of catalyst metal impurities on the TC of diamond is weaker, as they are distributed mainly in the form of inclusions inside the diamond particles.

Thermal conductivity of the composite

The maximal TCs of the composites we obtained from monodisperse fillers (diamond volume fraction of ~0.6) are shown in Table 6.

Comparing these results with the TC of diamond–metal composites obtained by other methods (infiltration or sintering, including the application of high pressure, above 1 GPa, or moderate pressure, less than 100 MPa, from Cu–Cr, Cu–B, and Ag–Si alloys [10–15]), and taking into account the effect of diamond particle size, one may conclude that the TC values of the composites we obtained are among the highest known to date.

Thermal resistance of the coating

Within the model of isolated inclusions imbedded into a matrix, we use

- the Hasselman–Johnson Eq. 11, deduced in the Maxwell mean field (MMF) scheme [47];
- Equation 12, deduced in the differential effective medium (DEM) scheme [22].

$$A = \frac{2\left(\frac{\lambda_d}{\lambda_m} - B - 1\right)v_d + \left(\frac{\lambda_d}{\lambda_m} + 2B + 2\right)}{\left(1 - \frac{\lambda_d}{\lambda_m} + B\right)v_d + \left(\frac{\lambda_d}{\lambda_m} + 2B + 2\right)} \tag{11}$$

$$1 - v_d = \frac{\varphi - A}{\varphi - 1}A^{-1/3} \tag{12}$$

Table 6 Experimental maximal TC of composites λ^{max} and calculated heat conductance G of the diamond-metal interface

Matrix	Diamond	Particles mean size D (μm)	Coating thickness h (nm)	λ^{max} (W m^{-1} K^{-1})	G[a] (W m^{-2} K^{-1})	
					MMF	DEM
Cu	SDB 1085	430	110	910	>3 × 10^7	1 × 10^8
	AS-160	180	240	770	6 × 10^7	5 × 10^7
Ag	SDB 1085	430	110–240	830–850	4 × 10^7	3 × 10^7
	AS-160	180	130	650	2 × 10^7	2 × 10^7

[a] *MMF* calculation by Eq. 11, *DEM* by Eq. 12

where $A = \lambda/\lambda_m$; $B = 2\lambda_d/(GD)$; $\varphi = \lambda_d/[\lambda_m(1 + B)]$; λ, λ_m, λ_d, W m^{-1} K^{-1} are the TC of composite, matrix, and diamond, respectively; v_d is the volume fraction of the diamond; D (m) is the diamond particle diameter; G (W m^{-2} K^{-1}) is the heat conductance of the filler/matrix interface.

In using these equations, we take account of the fact that the coating thickness is far less than the particle diameter and treat the coating layer together with the diamond/coating and coating/matrix interfaces as one total interface.

Until recently the Hasselman–Johnson Eq. 11 was the most popular for calculating interface heat conductivity on the basis of the experimental TC of diamond–metal composites. However, it was demonstrated by comparative calculations [22], that the DEM model gives more adequate values of G for diamond–metal composites than the MMF approach.

We calculated the heat conductance of the filler–matrix interface in the diamond–metal composites obtained from the maximal values of TC achieved (see Table 1), assuming $\lambda_d = 1500$ W m^{-1} K^{-1}. The results are listed in Table 6. The measured TC of the SDB 1085—Cu composite $\lambda^{max} = 910$ W m^{-1} K^{-1} is equal to the TC value calculated by the Maxwell equation ($B = 0$ in Eq. 11, zero thermal resistance of the interface). This validates that the DEM approach is more correct for the evaluation of G.

Comparative data on interface heat conductance in composites of diamond fillers with metal matrices are presented in Table 7.

As can be seen, the values we achieved for interface heat conductance, (2–10) × 10^7 W m^{-2} K^{-1}, in diamond–W–Cu and diamond–W–Ag composites made from pre-coated diamonds with tungsten, are close to or higher than those measured for composites obtained by other methods. It must be borne in mind that the calculations using the MMF approach by other authors give overestimated values for G.

Coefficient of thermal expansion

The CTE of 6.9–9.7 ppm/K for the composites we obtained (Table 1) has an intermediate value, between the corresponding coefficients of the filler and binder materials, and is close to the CTE of composites of similar composition obtained by other methods. Thus, at temperatures of 300–600 K, $\alpha = 1.0$–3.1 ppm/K for diamond, 16.7–18.7 ppm/K for copper and 18.9–21.0 ppm/K for silver [25, 28, 33]. A diamond–copper composite without a third

Table 7 Heat conductance, G, of the filler/matrix interface in diamond-metal composites with high thermal conductivity

Composite	Method of obtaining		Calculation		Source
	Process[a]	Raw[b]	G (W m^{-2} K^{-1})	Model	
Diamond/W/Cu	I	Cu	(5–10) × 10^7	DEM	This work
Diamond/W/Ag		Ag	(2–3) × 10^7		
Diamond/Cu	HPS	Cu	3.0 × 10^7	MMF	[10]
Diamond/Cr/Cu	FS	Cu–0.8% Cr	3.5 × 10^7	MMF	[14]
Diamond/Cr/Cu		Cu–0.8% Cr	9.4 × 10^7		[15]
Diamond/Cu[c]		Cu	<1 × 10^6		[15]
Diamond/Si/Ag	GPI	Ag–3% Si	6.6 × 10^7	DEM	[13]
Diamond/Al	GPI	Al	5 × 10^7		
Diamond/Al	GPI	Al	1.8 × 10^8	MMF	[7]

[a] *I* infiltration, *HPS* sintering under high pressure, *FS* fast sintering under pressure, *GPI* gas pressure assisted infiltration; for more details on references see "Introduction"

[b] For alloys, the mass fraction of the carbide-forming addition is specified

[c] Composite with a low thermal conductivity

component, with a diamond particle size of 40–60 μm and a diamond volume fraction of 0.60, had a CTE of 9.0 ppm/K [10].

Conclusions

A method has been developed of obtaining diamond–metal composites with high thermal conductivity, using a matrix from metals of the IB Group of Periodic Table, which includes the following stages: (1) prior deposition of a single-layered tungsten coating on a diamond powder and (2) infiltration of a metal melt (Cu, Ag) into a dense bed of coated diamond particles. For monodisperse filler ($v_d \sim 0.6$) of synthetic diamond with an average particle size of 430 or 180 μm, the composites obtained have a low porosity and a thermal conductivity of up to 900 W m^{-1} K^{-1}. Meanwhile, in various series of samples, both a predictable decrease in the TC of the composite with an increase of the coating thickness, h, and an unusual increase (constancy) in TC with increasing h were observed.

The optimal values of coating thickness h for forming composites with maximal TC are 100–250 nm. This range of optimal thickness is limited by or close to the threshold values for h below which it is not possible to produce a composite by pressureless infiltration. The heat conductance of the filler/matrix interface in these diamond–W–Cu and diamond–W–Ag composites is (2–10) × 10^7 W m^{-2} K^{-1} according to calculations using the DEM model.

The composite TC and interface heat conductance achieved are at the level or exceed values known hitherto for composites with similar diamond fillers, obtained by other techniques.

Analysis of data on thermal conductivity and wetting angles for metals and carbides shows that tungsten is the only element (with the possible exception of molybdenum) for formation of coatings on diamond to make diamond–metal composites with a high thermal conductivity by a spontaneous infiltration.

Acknowledgements Authors express their appreciation to E.A. Sosnov (St.Petersburg State Institute of Technology) for AFM analysis. Partly this study (S.V. Kidalov and F.M. Shakhov) was supported by the Russian Foundation for Basic Research (RFBR) grant 09-08-01200-a.

References

1. Shinde SL, Goela JS (eds) (2006) High thermal conductivity materials. Springer, New York
2. Zweben C (1998) J Miner Met Mater Soc 50:47
3. Prieto R, Molina JM, Narciso J, Louis E (2008) Scripta Mater 59:11
4. Kidalov SV, Shakhov FM (2009) Materials 2(4):2467
5. Gordeev SK, Zhukov SG, Danchukova LV, Ekstrom TC (2001) Neorganicheskie Materialy 37:691 [(2001) Low-pressure fabrication of diamond–SiC–Si composites. Inorg Mater 37:579–583]
6. Park JS, Sinclair R, Rowcliffe D, Stern M, Davidson H (2006) J Mater Sci 41:4611. doi:10.1007/s10853-006-0249-7
7. Ruch PW, Beffort O, Kleiner S, Weber L, Uggowitzer PJ (2006) Compos Sci Technol 66:2677
8. Hanada K, Matsuzaki K, Sano T (2004) J Mater Process Technol 153–154:514
9. Barcena J, Maudes J, Vellvehi M, Jorda X, Obieta I, Guraya C, Bilbao L, Jimenez C, Merveille C, Coleto J (2008) Acta Astronaut 62:422
10. Yoshida K, Morigami H (2004) Microelectron Reliab 44:303
11. Yekimov EA, Suetin NV, Popovich AF, Ralchenko VG, Gromnitskaya EL, Modenov VP (2008) Neorganicheskie Materialy 44:275 [(2008) The influence of microstructures and particle dimensions on the thermal conductivity of diamond composites obtained at high pressures. Inorg Mater 44:224–229]
12. Weber L, Tavangar R (2007) Scripta Mater 57:988
13. Weber L, Tavangar R (2009) Adv Mater Res 59:111
14. Schubert T, Ciupinski L, Zielinski W, Michalski A, Weibgarber T, Kieback B (2008) Scripta Mater 58:263
15. Schubert T, Trindade B, Weibgarber T, Kieback B (2008) Mater Sci Eng A 475:39
16. Kerns J, Colella N, Makowiecki D, Davidson H (1995) In: International symposium on microelectronics, Los Angeles, October 24–26, 1995. http://www.osti.gov/bridge/purl.cover.jsp?purl=/112941-Ymk33a/webviewable/
17. Kerns J, Colella N, Makowiecki D, Davidson H (1996) Int J Microcircuits Electron Packag 19:206
18. Chu K, Liu Z, Jia C, Chen H, Liang X, Gao W, Tian W, Guo H (2010) J Alloys Compd 490:453
19. Xia Y, Song Y, Lin C, Cui S, Fang Z (2009) Trans Nonferrous Met Soc China 19:1161
20. Novikov NV, Gontar' AG (1990) In: Kvaskov VB (ed) Almaz v elektronnoi tehnike. Energoatomizdat, Moskow (in Russian) [Application of synthetic diamonds in electronics. In: Diamond in electronic technology]
21. Abyzov AM, Kidalov SV, Shakhov FM (2008) Materialovedenie 5:24 [(2008) Composite material of diamond-copper with high thermal conductivity. Mater Sci Trans 5:24–27]
22. Tavangar R, Molina JM, Weber L (2007) Scripta Mater 56:357
23. Chuprina VG (1992) Poroshkovaya Metallurgiya 7:34 [(1992) Physicochemical interaction and structure development during the formation of metal gas-transfer coatings on diamond (review). I. Kinetics. Powder Metall Met Ceram 31(7):578–583]
24. Chuprina VG (1992) Poroshkovaya Metallurgiya 8:57 [(1992) Physicochemical interaction and structure development during the formation of metal gas-transport coatings on diamond (review). II. Mechanism. Powder Metall Met Ceram 31(8):687–692]
25. Osintsev OE, Fedorov VN (ed) (2004) Med' i mednye splavy. Mashinostroenie, Moskow (in Russian) [Copper and copper alloys]
26. International Tables for Crystallography (2006) vol C, chapt 4.2
27. Kunii D, Levenspiel O (1969) Fluidization engineering. Wiley, New York
28. Novikov NV (ed) (1987) Fizicheskie svoistva almaza. Naukova dumka, Kiev (in Russian) [Physical properties of diamond]
29. Naidich YuV (ed) (1991) Poverhnostnye svoistva rasplavov i tverdyh tel I ih ispol'zovanie v materialovedenii. Naukova dumka, Kiev (in Russian) [Surface properties of melts and solids and their application in materials technology]
30. Naidich YuV, Lavrinenko IA, Evdokimov VA (1974) Poroshkovaya Metallurgiya 1:34 [(1974) Densification in liquid phase

sintering under pressure in the system tungsten-copper. Powder Metall Met Ceram 13(1):26–30]
31. Kosolapova TYa (ed) (1986) Svoistva, poluchenie i primenenie tugoplavkih soedinenii. Metallurgiya, Moskow (in Russian) [Properties, making and application of refractory substances]
32. Mortimer DA, Nicholas M (1973) J Mater Sci 8:640. doi: 10.1007/BF00561219
33. Grigor'ev IS, Meilihov EZ (eds) (1991) Fizicheskie velichiny. Energoatomizdat, Moskow (in Russian) [Physical quantities]
34. Cardarelli F (2008) Materials handbook, chap 3. Springer, London, p 10
35. Eremenko VN, Minakova RV, Churakov MM (1977) Poroshkovaya Metallurgiya 4:53 [(1977) Solubility of tungsten in copper-nickel melts. Powder Metall Met Ceram 16(4):283–286]
36. Abrikosov NH (ed) (1979) Dvoinye i mnogokomponentnye sistemy na osnove medi. Nauka, Moskow (in Russian) [Binary and multicomponent systems on the copper basis]
37. Dorfman S, Fuks D, Suery M (1999) J Mater Sci 34:77. doi: 10.1023/A:1004461423717
38. Bhushan B (2007) In: Bhushan B (ed) Springer handbook of nanotechnology. Springer, Berlin Heidelberg
39. Yang B, Chen G (2004) In: Tritt T (ed) Thermal conductivity: theory, properties and applications. Kluwer Academic/Plenum Publishers, New York
40. Feng B, Li Z, Zhang X (2009) Thin Solid Films 517:2803
41. Efimov VB, Mezhov-Deglin LP (1999) Physica B 263–264:745
42. Naidich YuV, Kostyuk BD, Kolesnichenko GA, Shaikevich SS (1973) Poroshkovaya Metallurgiya 12:55 [(1973) Adhesion properties and wetting by molten metals of thin metallic films applied to nonmetallic materials. Powder Metall Met Ceram 12(12):988–993]
43. Naidich YuV, Volk GP, Lavrinenko IA (1981) Poroshkovaya Metallurgiya 9:22 [(1981) Infiltration of metal-coated diamond powders by molten metal. Powder Metall Met Ceram 20(9): 610–612]
44. Marmur A (2009) Annu Rev Mater Res 39:473
45. Nicholas M, Poole DM (1967) J Mater Sci 2:269. doi:10.1007/BF00555384
46. Kornilov II, Glazova VV (1967) Vzaimodeistvie tugoplavkih metallov perehodnyh grupp s kislorodom. Nauka, Moskow (in Russian) [Interaction of refractory metals of transition groups with oxygen]
47. Hasselman DPH, Johnson LF (1987) J Compos Mater 21:508